Preprints of the 21st IFAC World Congress (Virtual)
Berlin, Germany, July 12-17, 2020

Shaft Speed Control of the Gas Turbine Based on Active Disturbance Rejection Control

Gengjin Shi* Zhenlong Wu* Ting He Donghai Li* Yanjun Ding* Shangming Liu*****
State Key Lab of Power Systems, Department of Energy and Power Engineering, Tsinghua University, Beijing, 100084 China (e-mails: sgj18@mails.tsinghua.edu.cn (Shi, G.); wu-zl15@mails.tsinghua.edu.cn (Wu, Z.); dyj@tsinghua.edu.cn (Ding, Y.); Corresponding author: **Donghai Li; e-mail: lidongh@tsinghua.edu.cn)*
***Energy and Electricity Research Center, International Energy College, Jinan University, Zhuhai, 519070 China (e-mail: heting@jnu.edu.cn)*
****Institute of Gas Turbines, Department of Energy and Power Engineering, Tsinghua University, Beijing, 100084 China (e-mail: liushm@tsinghua.edu.cn)*

Abstract: As a clean energy engine, the gas turbine has many challenges in its shaft speed control such as strong nonlinearity and various external disturbances. However, conventional controllers such as proportional-integral-derivative (PID) controllers are not able to obtain satisfactory performance in disturbance rejection when the operating point is changing. To handle with the strong nonlinearity and reject possible disturbances more effectively, the linear active disturbance rejection controller (LADRC) is applied to the shaft speed control system of the gas turbine based on an experimental tuning procedure. Moreover, Skogestad Internal Model Control-PID (SIMC-PID) and fractional order PID (FOPID) are chosen as comparative controllers. Eventually, Monte Carlo trials are carried out and maximum sensitivities are calculated in order to test the robustness of controllers. Simulation results illustrate the advantages of LADRC in both reference tracking and rejections of different disturbances.

Keywords: Gas turbine, Shaft speed control, Linear active disturbance rejection control, Robustness test, Monte Carlo trials.

1. INTRODUCTION

The gas turbine (GT) is a typical internal combustion engine which is widely used in modern industry (Singh R. et.al. 2018). It consists of the compressor, the combustion chamber and the turbine. In terms of their structures, gas turbines are divided into three categories: the heavy-duty gas turbine (HDGT), the light-duty gas turbine (LDGT) and the micro gas turbine (MGT). The HDGT is mostly applied to power generation for its high efficiency and long service life.

In a power generation system with the gas turbine, the output shaft of the prime motor is connected with the shaft of generator. Driven by the same shaft, the generator and the gas turbine mutually complete the conversion of mechanical energy to electricity. Therefore, the control of shaft speed is of significance for a gas turbine. Previous studies were proposed in the past decade. D. Yan *et al* optimized the parameters of the controller based on neural network algorithm. In this case the controller has the adaptability to the change of working conditions (Yan D. et.al. 2008). Z. Wang designed a fuzzy proportional-integral-derivative (PID) controller for the control system of shaft speed. Simulation results indicated that using fuzzy algorithm was able to obtain meaningful results (Wang Z. 2009). In addition, many advanced control strategies are applied to the shaft speed control of GT such as model predictive control (MPC). (Sun H. 2015).

However, these advanced control strategies are difficult for applications in field tests for the reason that they are difficult to implement on the distributed control system (DCS). Nowadays, PID controllers are commonly used in control systems of gas turbines. But their hysteretic regulating characteristics limit the response speed of the system (Si W. 2016). Using conventional control strategies, the GT is not responsive for the reason that there are various disturbances from the outside such as the fluctuation of air temperature, the quality decline of the fuel and the ascent of the valve opening. Hence it is necessary to find a simple controller which is able to obtain the better performance than PID controller in the control of shaft speed.

Active disturbance rejection control (ADRC), proposed by Chinese scholar J. Han (Han J. 2009), is regarded as the successor of PID controller in industrial automation fields. Its core idea is that uncertainties, modelling errors and disturbances are all considered as an extended state which is estimated and compensated by an observer (Shi G. et.al. 2019). ADRC inherits the advantages of PID controller and has less dependency on the explicit model of the system. However, the nonlinear form is unavailable for the configuration of DCS in industrial processes because its tuning is complicated. To solve this problem, Z. Gao simplified ADRC into linear form (Gao Z. 2003) and standardized its tuning based on bandwidth-parameterization. This simplification enabled ADRC to be applied to solve problems in engineering. In the past decades, the linear ADRC (LADRC) has been widely used in industrial processes such as superheated steam temperature (Wu Z. et.al. 2018; Shi G. et.al. 2020), proton exchange membrane fuel cell (Sun, L. et.al. 2018) and fluidized bed combustor (Wu Z. et.al. 2020), which shows its developing prospects in thermal engineering.

In this paper, LADRC is applied to the shaft speed control system of a typical gas turbine in order to handle with the strong nonlinearity and improve the performance of the

disturbance rejection. To highlight the advantages of LADRC, we select PID based on Skogestad Internal Model Control (SIMC-PID) and fractional order PID (FOPID) as the comparative controllers. Besides, Monte Carlo method is used to evaluate controllers from both dynamic performance and robustness. Finally, concluding remarks are offered in the last section.

2. MECHANISM MODEL OF THE GAS TURBINE

Fig. 1 presents the configuration of the gas turbine. The mechanism model was established based on the first law of thermodynamics, conversion of mass, heat transfer equations and heat balance equations (Sun W. 2016).

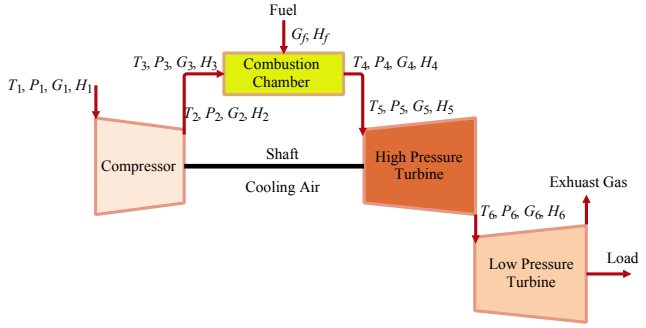

Fig. 1. The configuration of a gas turbine.

To simplify the mechanism model of the gas turbine, several assumptions are made before modelling:

- Ignore the influence of altitude.
- Ignore the thermal inertia of all components and the combustion delay.
- The flow of gas in the gas turbine is regarded as one-dimensional flow.
- The working medium is considered as ideal gas.
- Compression and expansion of gas are approximated as adiabatic processes.
- Constant thermo-physical properties are assumed such as the air constant (γ_{air}), the gas constant (γ_{gas}) and lower heating value of the fuel (LHV).
- All volumes are constant.

The model is divided into two parts: the static model and dynamic model. The former one includes the compressor, the combustion chamber, the high pressure turbine and the low pressure turbine while the latter one consists of the rotor. In this paper, P, T, G and H represent pressure, temperature, the rate of flow and enthalpy, respectively. As for the ideal gas, the enthalpy is the monotropic function of the temperature,

$$H = f(T). \tag{1}$$

Compressor: The compressor map is two-dimensional. The efficiency (η_c) and the corrected mass flow rate (G_c) of compressor are able to be evaluated by the map,

$$\left(\frac{\sqrt{T_1}}{P_1}, \frac{n}{\sqrt{T_1}}\right) \xrightarrow{compressor\ map} \left(G_c, \eta_c\right), \tag{2}$$

$$T_2 = T_1\left\{1+\frac{1}{\eta_c}\left[\left(\frac{P_2}{P_1}\right)^{\frac{\gamma_{air}-1}{\gamma_{air}}}-1\right]\right\}, \tag{3}$$

$$P_c = G_c\left(H_2 - H_1\right), \tag{4}$$

where n represents the shaft speed. P_c refers to the power of the compressor.

Combustion Chamber: In Fig. 1, G_f and H_f refers to the flow rate and enthalpy of the fuel, respectively. The pressure of the gas (P_4) and the heat balance in the chamber are depicted as follows,

$$P_4 = \sigma_{cb} \bullet P_3, \tag{5}$$

$$G_4H_4 = G_3H_3 + G_f\left(H_f + \eta_{cb} \bullet LHV\right), \tag{6}$$

where σ_{cb} is denoted as the combustion pressure recovery factor. η_{cb} is defined as the efficiency of combustion.

Turbines: In this section, we take high pressure turbine (HPT) as an example for the reason that the low pressure turbine (LPT) has the same properties with HPT. The efficiency (η_{hpt}) and the corrected mass flow rate (G_{hpt}) of HPT are able to be obtained by the two-dimensional turbine map,

$$\left(\frac{\sqrt{T_5}}{P_5}, \frac{n}{\sqrt{T_5}}\right) \xrightarrow{turbine\ map} \left(G_{hpt}, \eta_{hpt}\right), \tag{7}$$

$$T_6 = T_5\left[1-\left(\frac{P_6}{P_5}\right)^{\frac{\gamma_{gas}-1}{\gamma_{gas}}}\right]\eta_{hpt}, \tag{8}$$

$$P_{hpt} = G_{hpt}\left(H_6 - H_5\right), \tag{9}$$

where P_{hpt} refers to the power of HPT.

Rotor: The variations of shaft speed are caused by the power imbalance of the compressor and the high pressure turbine,

$$\frac{dn}{dt} = \frac{900}{\pi^2 Jn}\left(P_{hpt} - P_c\right), \tag{10}$$

where J is denoted as the moment of inertia of the rotor.

In order to complete iterative calculations in the model, we set several initial parameters which are shown in Table 1. This mechanism model is established on the platform of MATLAB Simulink.

Table 1. Initial parameters

Parameters	Symbol	Value
Ambient pressure (kPa)	P_0	101.325
Ambient temperature (K)	T_0	288.15
Pressure recovery factor	σ_{cb}	0.98
Combustion efficiency	η_{cb}	0.99
Lower heating value (kJ/kg)	LHV	48952
Initial flow rate of fuel (kg/s)	G_{f0}	1.795
Initial shaft speed (rpm)	n_0	9806
Moment of inertia (kg·m^2)	J	3039.6

3. CONTROL DIFFICULTIES ANALYSIS

In the gas turbine, components are connected by pipes which may form strong nonlinearities. Therefore, the dynamic characteristic of the system varies significantly at different operating points. Fig. 2 shows open-loop responses of the system at three different working conditions under a negative step input signal. N is denoted as the load. In this section, gap metric is applied to the shaft speed system in order to analyze the nonlinearity of the shaft speed system and it is regarded as a measurement of the distance between two linear time invariant (LTI) systems (Yuan J. et.al. 2019).

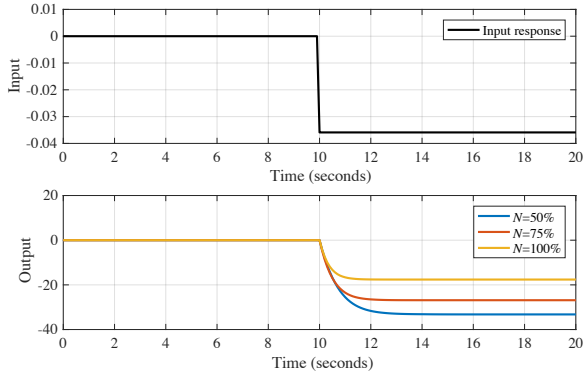

Fig. 2. Open-loop responses at different working conditions.

The gap between two systems is defined as,

$$Gap\left(G_1,G_2\right)=\max\left[\vec{\delta}\left(G_1,G_2\right),\vec{\delta}\left(G_2,G_1\right)\right], \tag{11}$$

where G_1 and G_2 are transfer functions linearized around the nominal working condition and $\vec{\delta}(G_1, G_2)$ represents the direct gap which is defined as,

$$\vec{\delta}\left(G_1,G_2\right)=\inf_{A\in H_\infty}\left\|\begin{bmatrix}P_1\\Q_1\end{bmatrix}-\begin{bmatrix}P_2\\Q_2\end{bmatrix}A\right\|, \tag{12}$$

where $G_1=Q_1P_1^{-1}$ and $G_2=Q_2P_2^{-1}$. A is a matrix parameter which has H_∞ form. The gap is restricted as follow,

$$0\le\vec{\delta}\left(G_1,G_2\right)\le 1. \tag{13}$$

The high value of gap means strong nonlinearity and vice versa. In this section, let G_1 represents the transfer function of nominal working condition which is chosen as 50% load. The gap is plotted as Fig. 2.

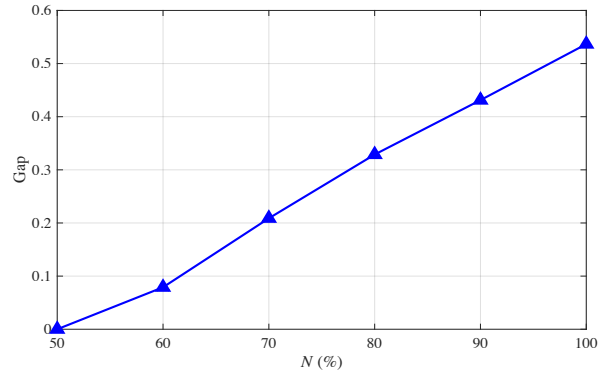

Fig. 3. Gap measurement at different operating points.

In Fig. 3, it is obvious that the gap is big when the load is high. Therefore, the shaft speed system has a strong nonlinearity.

Moreover, note that the range of working conditions in this nonlinear system is $N\in[31, 100]$. If the operating point is out of the range, the simulation will terminate.

4. DESIGN OF SHAFT SPEED CONTROL SYSTEM

The shaft speed of the gas turbine is the main output of the control system because it determines the power generation. In the control system of a gas turbine, the control of exhaust temperature and shaft speed acceleration is subordinate (Rowen W. 1983). Therefore, the control system of the gas turbine is able to be simplified as Fig. 4.

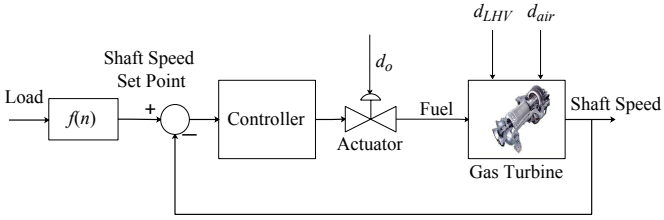

Fig. 4. Block diagram of the shaft speed control system.

The shaft speed set point is determined by the load. In Fig. 4, d_o, d_{LHV} and d_{air} are defined as disturbances caused by valve opening, LHV and inlet air temperature, respectively.

4.1 Actuator

The shaft speed is determined by the energy in the fuel. In the system shown in Fig. 5, the shaft speed is controlled by regulating the opening of fuel valve. The model of the valve can be depicted as a first order plus dead time (FOPDT) transfer function (Dorf R.C. et.al. 2011),

$$G_{valve}(s)=\frac{K}{Ts+1}e^{-\tau s}. \tag{14}$$

Parameters in $G_{valve}(s)$ are able to be obtained using two points method (Cvejn J. 2011). In this paper, the parameters are chosen for simulation as,

$$K=7.2\times10^{-5},\ T=0.565,\ \tau=0.088.$$

4.2 Introduction of Linear ADRC

In this paper, we apply the second-order linear ADRC to the shaft speed control system of the gas turbine. Suppose that the process is considered as a general second order system,

$$\ddot{y}=g\left(t,y,\dot{y},\ddot{y}\cdots,d\right)+bu, \tag{15}$$

where $g\left(t,y,\dot{y},\ddot{y}\cdots,d\right)$ refers to the synthesis of external disturbances, high order dynamics and modelling error of the system. u is denoted as the input while y is defined as the output. b is regarded as the critical gain (Sun L. et.al. 2017), whose value may be unknown. As a result, Equation (15) is able to be rewritten as,

$$\ddot{y} = b_0 u + f \,, \tag{16}$$

where b_0 is the estimation of the critical gain and f refers to the total disturbance of the system which is derived as $f=g+(b-b_0)$. Let the state vector of the process $\boldsymbol{x}=[x_1\ x_2\ x_3]^T=[y\ \mathrm{d}y/\mathrm{d}t\ f]^T$, where x_3 is regarded as the extended state. Therefore, the state-space expression of the process is depicted as,

$$\begin{cases} \dot{\boldsymbol{x}} = \boldsymbol{A}\boldsymbol{x} + \boldsymbol{B}u + \boldsymbol{\lambda}\dot{f} \\ y = \boldsymbol{C}\boldsymbol{x} \end{cases}, \tag{17}$$

where $\boldsymbol{A}=\begin{bmatrix} 0 & 1 & 0 \\ 0 & 0 & 1 \\ 0 & 0 & 0 \end{bmatrix}$, $\boldsymbol{B}=\begin{bmatrix} 0 \\ b_0 \\ 0 \end{bmatrix}$, $\boldsymbol{\lambda}=\begin{bmatrix} 0 \\ 0 \\ 1 \end{bmatrix}$ and $\boldsymbol{C}=\begin{bmatrix} 1 & 0 & 0 \end{bmatrix}$.

The extended state observer (ESO) is designed as,

$$\dot{\boldsymbol{z}} = \boldsymbol{A}\boldsymbol{z} + \boldsymbol{B}u + \boldsymbol{L}\left(y - z_1\right), \tag{18}$$

where $\boldsymbol{z}=[z_1\ z_2\ z_3]^T$ and $\boldsymbol{L}=[\beta_1\ \beta_2\ \beta_3]^T$ represent the state vector and the gain vector of the observer, respectively. If $\boldsymbol{L}$ is set appropriately, $\boldsymbol{z}$ is able to track $\boldsymbol{x}$ accurately (Guo B. et.al. 2011).

The state feedback control law (SFCL) is depicted as,

$$u = \frac{k_p\left(r - z_1\right) - k_d z_2 - z_3}{b_0}. \tag{19}$$

where r represents the reference signal; k_p and k_d are the tunable parameters of the SFCL. Fig. 5 shows the block diagram of the second-order LADRC.

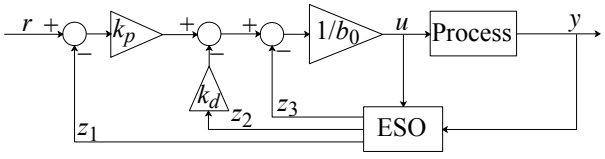

Fig. 5. The block diagram of the second order LADRC.

According to the design of LADRC, it is obvious that the total disturbance of the system is able to be estimated by ESO and eliminated by SFCL. Therefore, LADRC has the ability to compensate uncertainties of the process.

The second order LADRC has six tunable parameters which makes its tuning procedure complex. In order to solve this problem, Z. Gao summarized a tuning method for the second order LADRC based on bandwidth-parameterization (Gao Z. 2003). The process is reduced to a unit gain double integrator,

$$\ddot{y} = \left(f - z_3\right) + u_0 \approx u_0 \,. \tag{20}$$

If the parameters of ESO are chosen appropriately, the closed-loop characteristic polynomial is able to be written as,

$$\ddot{y} + k_d\dot{y} + k_p y = k_p r \,, \tag{21}$$

$$T\left(s\right) = s^2 + k_d s + k_p = \left(s + \omega_c\right)^2, \tag{22}$$

where ω_c is denoted as the bandwidth of the feedback control system. Therefore, k_p and k_d are evaluated as,

$$k_p = \omega_c^{\,2},\ k_d = 2\omega_c \,. \tag{23}$$

The characteristic polynomial of ESO can be written as,

$$s^3 + \beta_1 s^2 + \beta_2 s + \beta_3 = \left(s + \omega_o\right)^3, \tag{24}$$

where ω_o is denoted as the bandwidth of the observer. The parameters of ESO can be depicted as,

$$\beta_1 = 3\omega_o,\ \beta_2 = 3\omega_o^{\,2},\ \beta_3 = \omega_o^{\,3} \,. \tag{25}$$

The tuning procedure of LADRC is based on following two principles:

(a) With the increase of ω_o, the observer velocity of ESO will increase. As a result, ω_o increases from a low value until the observing precision is satisfactory. Generally, we let ω_o=3~5ω_c (Gao Z. 2003); **(b)** With the increase of ω_c and the decrease of b_0, the response of system will be faster but the overshoot will be larger and the oscillation will be fiercer.

Note that the LADRC is a linear controller. In this paper, it is applied to the nonlinear mechanism model which has been established in Section 2.

4.2 Introductions of Comparative Controllers

In order to illustrate advantages of LADRC in both reference tracking and disturbance rejection, we select SIMC-PID and FOPID as comparative controllers.

SIMC-PID: The PID controller has the form as follow,

$$G_{PID}\left(s\right) = K_P\left(1 + \frac{1}{T_i s} + T_d s\right). \tag{26}$$

SIMC-PID tuning method was proposed by S. Skogasted (Skogestad S. 2003). The process is estimated as a second-order plus dead time (SOPDT) transfer function,

$$G_p\left(s\right) = \frac{K}{\left(T_1 s + 1\right)\left(T_2 s + 1\right)} e^{-\tau s}. \tag{27}$$

The parameters of PID controller are tuned as,

$$\begin{aligned} K_P &= \frac{1}{K}\frac{T_1}{T_c + \tau} \\ T_i &= \min\left\{T_1, 4\left(T_c + \tau\right)\right\} \\ T_d &= T_2 \end{aligned}, \tag{28}$$

where T_c refers to the desired time constant of the process.

FOPID: FOPID controller was first proposed and analysed in the frequency domain by I. Podlubny (Podlubny I. 1994). It has the form as,

$$G_{FOPID}(s) = K_P\left(1+\frac{1}{T_i s^{\lambda}}+T_d s^{\mu}\right). \tag{29}$$

H. S. Sanchez et al derived a tuning method of FOPID based on multi-objective optimization (Sánchez H.S. et.al. 2017). The process is estimated as a FOPDT transfer function shown in (10). The tuning rules are as follows,

$$\begin{aligned} K_P &= \frac{1}{K}\left(0.7256\tau^{-1.0221}+0.3064\tau^{-0.0624}\right)\\ T_i &= T^{\lambda}\left(-0.0900\tau^2+0.8472\tau+0.5113\right)\\ T_d &= T^{\mu}\left(-0.0273\tau^2+0.3198\tau-0.0075\right)\\ \mu &= -0.0343\tau+1.1403\\ \lambda &= 1 \end{aligned}. \tag{30}$$

According to the tuning methods in this section, the parameters of LADRC, SIMC-PID and FOPID are taken as Table 2.

Table 2. Parameters of controllers

Controller	Parameters
LADRC	ω_c=1.0014, ω_o=4.0096, b_0=0.1199
SIMC-PID	K_P=3.6702, T_i=1.4793, T_d=0.0026
FOPID	K_P=0.5421, T_i=0.0799, T_d=1.1401, μ=1.0877, λ=1

5. SIMULATION RESULTS

During simulation experiments, the operating point of gas turbine is changing during the simulation. The controller starts to work after 10 seconds. Suppose that there are disturbances caused by the valve opening, the fuel and the inlet air temperature after the shaft speed is stable at the set point.

The gas turbine is a nonlinear industrial plant which contains unpredictive uncertainties so that the robustness tests of controllers are vital. Monte Carlo trial is a practical method to test the robustness of a control system. It is able to intuitively indicate the system with which controller will obtain the strongest robustness and best dynamic performance.

We expect that the output of shaft speed control system has the smallest overshoot (or undershoot), the shortest settling time and the smallest integral of time multiplied by absolute error (ITAE) which is depicted as,

$$\text{ITAE}=\int_0^T t\left|e(t)\right|, \tag{31}$$

where $e(t)$ refers to the tracking error of the controlled variable and T is denoted as the simulation time. ITAE is a dynamic index to evaluate the control performance comprehensively.

Moreover, the strongest robustness is of necessity as well. In this paper, we the denote overshoot (or undershoot) and the settling time as σ and T_s, respectively. The settling time is calculated by ±2% principle.

5.1 Reference Tracking

Fig. 6 shows variations of the opening of fuel valve and the shaft speed of the gas turbine in first 70 seconds, respectively.

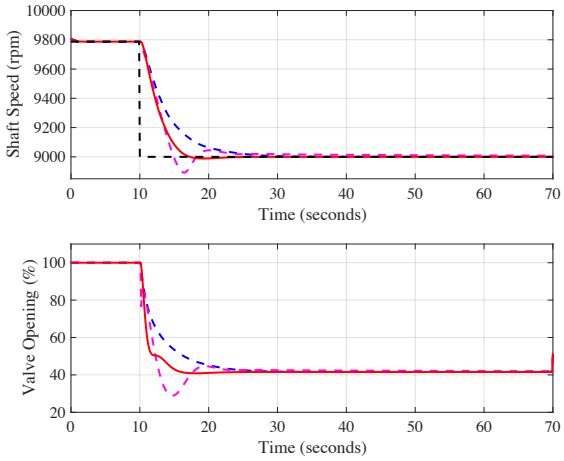

Fig. 6. Variations of shaft speed and valve opening in first 70 seconds (SIMC-PID:---, FOPID:---, LADRC:—, Set point:---).

In Fig. 6, although FOPID has the fastest reference tracking speed, it has an obvious undershoot and a tiny steady error. The undershoot of SIMC-PID is the smallest but its reference tracking speed is the slowest. Dynamic indices of reference tracking with different controllers are shown in Table 3, which are all recorded from 0s to 60s. According to Table 3, comparisons of dynamic performance in reference tracking among controllers are depicted as follow.

$$\begin{aligned} \sigma_{SIMC-PID} &< \sigma_{LADRC} < \sigma_{FOPID}\\ T_{s\_LADRC} &< T_{s\_SIMC-PID} < T_{s\_FOPID}\\ \text{ITAE}_{LADRC} &< \text{ITAE}_{FOPID} < \text{ITAE}_{SIMC-PID} \end{aligned}$$

Table 3. Dynamic indices of reference tracking

Controller	σ (%)	T_s (sec.)	ITAE
SIMC-PID	0	16.0	45739
FOPID	15.5	13.2	61654
LADRC	1.4	6.6	25346

5.2 Disturbance Rejection

Valve Opening: Assume that the control signal of the fuel valve is disturbed by other signals in the field so that the valve opening will step up. Fig. 7 shows the response of the shaft speed under the disturbance caused by valve opening.

In Fig. 7, it is obvious that LADRC is able to reject the disturbance in the shortest period. Compared with other controllers, FOPID still has a tiny steady error.

Lower Heat Value: Suppose that the fuel declines in quality which may influence the heat value of working medium. Fig. 8 shows the response of the shaft speed under the disturbance of LHV.

In Fig. 8, it is evident that FOPID has the best performance in the rejection of the disturbance of LHV. However, LADRC is able to recover to the set point fastest.

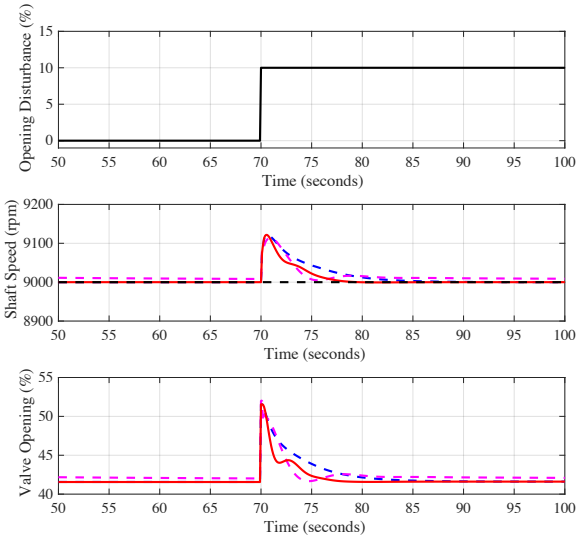

Fig. 7. Variation of shaft speed of the opening disturbance (SIMC-PID:---, FOPID:---, LADRC:—, Set point:---).

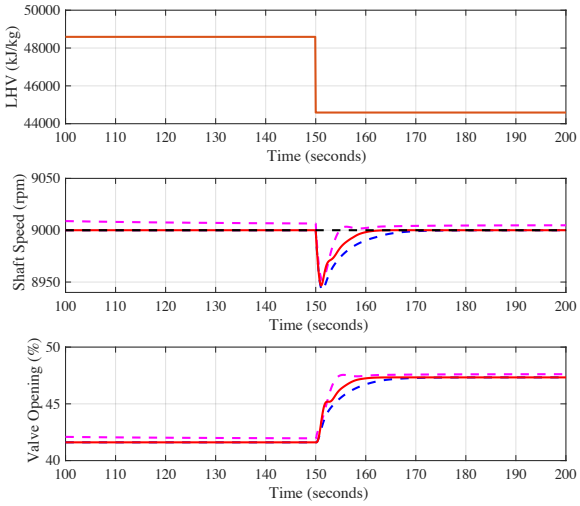

Fig. 8. Variation of shaft speed of the disturbance of lower heat value (SIMC-PID:---, FOPID:---, LADRC:—, Set point:---).

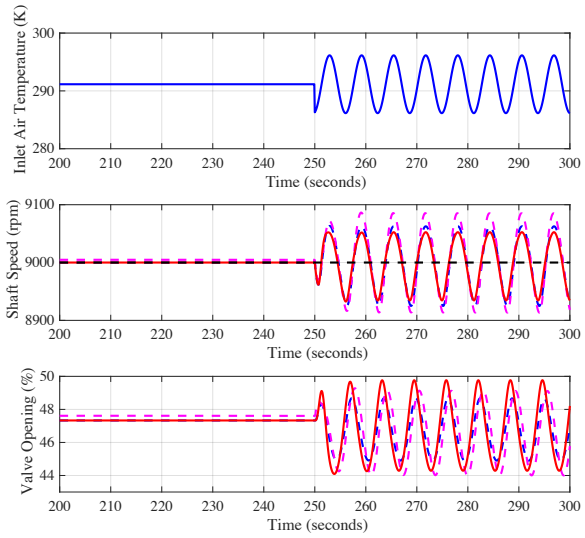

Fig. 9. Variation of shaft speed of the disturbance of the inlet air temperature (SIMC-PID:---, FOPID:---, LADRC:—, Set point:---).

Inlet Air Temperature: When the gas turbine is operating, the ambient temperature is changing which may disturb the shaft speed. Suppose that the disturbance of inlet air temperature is periodical. Fig. 9 shows the response of the shaft speed when the air temperature is fluctuating.

In Fig. 9, it is evident that the shaft speed has the smallest fluctuating amplitude under the periodical disturbance when LADRC is applied.

5.2 Robustness Test

The strong robustness means that a controller is able to obtain satisfactory control performance under the off-design working conditions. To test the robustness of controllers, we carry out 300 times of Monte Carlo trials. Fig. 10 shows the results.

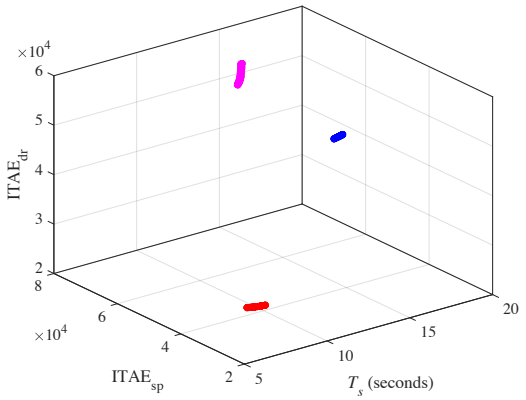

Fig. 10. Results of Monte Carlo trials (SIMC-PID: *, FOPID: *, LADRC: *).

$ITAE_{sp}$ and $ITAE_{dr}$ are defined as the ITAE of reference tracking and the valve opening disturbance rejection, respectively. The moment of inertia J fluctuates among ±10% of its nominal value in simulations, i.e. $J \in [2735.6, 3343.6]$. From Fig. 10, it is obvious that the SIMC-PID is more robust and has worse dynamic performance than LADRC. Compared with FOPID, LADRC has stronger robustness and smaller dynamic indices.

In order to further illustrate the advantage of LADRC in robustness, we calculate the maximum sensitivities (M_s) of the system with different controllers. The M_s is depicted as,

$$M_s = \max_{\omega} \left| \frac{1}{1+L(j\omega)} \right|, \omega \in (-\infty, +\infty), \tag{32}$$

where $L(j\omega)$ is denoted as the frequency characteristic of the open-loop transfer function and ω represents the frequency. Besides, j is regarded as the imaginary unit. If the M_s is smaller, the controller is more robust. For simplification, the controlled process is linearized around the working condition when the shaft speed is 9000 rpm. The system is identified as a first order process which is depicted as,

$$G(s) = \frac{17.2728}{0.79744s+1}. \tag{33}$$

Table 4 shows the M_s of different controllers under the aforementioned working condition. Note that M_s is able to be considered as the worst-case amplification of disturbances. Additionally, the reasonable range of M_s for control design is 1.0-2.5 (Astrom K. J. et.al. 2006).

Table 4. The M_s of different controllers

Controller	M_s
SIMC-PID	1.0053
FOPID	1.0105
LADRC	1.0074

According to Table 4, the comparison of maximum sensitivity among controllers is depicted as,

$$M_{s\_SIMC-PID} < M_{s\_LADRC} < M_{s\_FOPID}.$$

The M_s of LADRC is close to 1.0 which means that LADRC is robust with respect to the model parameter and structural uncertainties. Although the M_s of SIMC-PID is smaller than that of LADRC, the former controller has worse dynamic performance than latter one.

Generally speaking, in terms of the dynamic performance and robustness, LADRC is more suitable for the control of shaft speed.

6. CONCLUSIONS

To handle with the strong nonlinearity and reject various disturbances, LADRC is applied to the shaft speed control system of the gas turbine in this paper. The superiorities of LADRC in reference tracking and disturbance rejection are verified by numerical simulations. Moreover, Monte Carlo trials indicate that LADRC has advantages in both dynamic performance and robustness. The future work will focus on the field application of LADRC to the shaft speed control of the gas turbine.

ACKNOWLEDGEMENTS

The author would like to acknowledge the support of National Science and Technology Major Project (2017-V-0005-0055) of China and State Key Lab of Power Systems, Tsinghua University.

REFERENCES

Astrom, K. J. and Hagglund, T. (2006). *Advanced PID Control*, ISA Press Research Triangle Park, NC, USA.

Cvejn, J. (2011). Simple PI/PID controller tuning rules for FOPDT plants with guaranteed closed-loop stability margin. *Acta Montanistica Slovaca,* volume (16), 17-25.

Dorf, R.C., and Bishop, R.H. (2011). *Modern Control System Twelfth Edition,* Pearson Education, Inc., NJ, USA.

Gao, Z. (2003). Scaling and bandwidth-parameterization based controller tuning. *Proceedings of the American Control Conference,* 4989-4996.

Guo, B. and Zhao, Z. (2011). On the convergence of an extended state observer for nonlinear systems with uncertainty. *Systems & Control Letters,* volume (60), 420-430.

Han, J. (2009). *Active disturbance rejection control technique,* National Defense Industry Press, Beijing, China.

Podlubny, I. (1994). Fractional-order systems and $PI^{\lambda}D^{\mu}$ controllers. *IEEE Transaction on Automatic Control,* volume (44), 208-214.

Rowen, W. (1983). Simplified mathematical representation of heavy-duty gas turbines. *Journal of Engineering for Power,* volume (105), 865-869.

Sánchez, H., Padula, F. and Visioli, A. et.al. (2017). Tuning rules for robust FOPID controllers based on multi-objective optimization with FOPDT models. *ISA Transactions,* volume (66), 344-361.

Shi, G., He, T. and Wu, Z. et.al. (2019). Research on cascade active disturbance rejection control of superheated steam temperature based on gain scheduling. *Proceedings of 19th International Conference on Control, Automation and Systems,* 1426-1431.

Shi, G., Wu, Z. and Guo, J. et.al. (2020). Superheated steam temperature control based on a hybrid active disturbance rejection control. *Energies,* volume (13), 1757.

Si, W. (2016). Design and optimization on speed controller of gas turbine. *Master thesis,* Northeastern University.

Singh, R., Maity, A., and Nataraj, P.S.V. (2018). Modelling, simulation and validation of mini SR-30 gas turbine engine. *Proceedings of 5th IFAC Conference on Advances in Control and Optimization of Dynamical Systems,* 554-559.

Skogestad, S. (2003). Simple analytic rules for model reduction and PID controller tuning. *Journal of Process Control,* volume (13), 291-309.

Sun, H. (2015). Research of Multivariate sliding mode control on aero-engine. *Master thesis,* Tsinghua University.

Sun, L., Hua, Q. and Shen, J. et.al. (2017). Multi-objective optimization for advanced superheater steam temperature control in a 300 MW power plant. *Applied Energy,* volume (208), 592-606.

Sun, L., Shen, J. and Hua, Q. et.al. (2018). Data-driven oxygen excess ratio control for proton exchange membrane fuel cell. *Applied Energy,* volume (231), 866-875.

Sun, W. (2016). Simulation modelling and characteristic research of distributed energy system. *Master thesis*, Southeastern University.

Wang, Z. and Li, S. (2009). Simulation study on fuzzy PID control of gas turbine generating sets speed. *IEEE International Conference on Intelligent Computing,* 725-728.

Wu, Z., He, T. and Li, D. et.al. (2018). Superheated steam temperature control based on modified active disturbance rejection control. *Control Engineering Practice,* volume (83), 83-97.

Wu, Z., Li, D. and Xue, Y. et.al. (2020). Modified active disturbance rejection control for fluidized bed combustor. *ISA Transactions,* in press.

Yan, D., Yan, S. and Li, A. et.al. (2008). New neural network control of micro gas turbine. *Control Engineering of China,* volume (15), 541-548.

Yuan, J., Wu, Z. and Fei, S. et.al. (2019). Hybrid model-based feedforward and fractional-order feedback control design for the benchmark refrigeration system. *Industrial & Engineering Chemistry Research,* volume (58), 17889.